

## Interaction between electrostatic whistlers and electron holes in the auroral region

M. Berthomier, L. Muschietti, J. W. Bonnell, I. Roth, and C. W. Carlson

Space Sciences Laboratory, University of California, Berkeley, California, USA

Received 1 February 2002; revised 28 May 2002; accepted 7 June 2002; published 21 December 2002.

[1] Electron holes have been discovered in several key regions of the magnetosphere in the past few years. These small-scale structures seem to play an important role in the global dynamics of the magnetosphere, being most often associated with parallel electron beams and strong ion heating, as shown by the Fast Auroral Snapshot (FAST) spacecraft in the auroral region. Electrostatic whistler waves (EWW) in the VLF frequency range are often associated with these electron holes, suggesting that the generation of whistler waves is related to the holes. We present a model of the interaction between EWW and electron holes. Our analysis is based on the mechanical description of the energy exchange between particles and waves; by the use of the Hamiltonian formalism, action-angle variables, and canonical perturbation theory, we show that trapped electrons, owing to their periodic motion in the potential structure of the electron hole, enter into a resonance with the wave and can destabilize it at large parallel phase velocity relative to the electron thermal velocity. We derive the growth rate of EWW and compare our model with previous ones. Application to FAST observations shows that this linear instability is able to generate EWW with a normalized growth rate  $\gamma/\omega$  varying from a few percents at low frequency (above the lower-hybrid frequency) up to  $\sim 10\%$  at higher frequency (below the electron plasma frequency).

**INDEX TERMS:** 7815 Space Plasma Physics: Electrostatic structures; 7839 Space Plasma Physics: Nonlinear phenomena; 7867 Space Plasma Physics: Wave/particle interactions; 2704 Magnetospheric Physics: Auroral phenomena (2407); **KEYWORDS:** electrostatic whistlers, VLF saucers, electron holes, Hamiltonian plasmas, FAST observations, auroral regions

**Citation:** Berthomier, M., L. Muschietti, J. W. Bonnell, I. Roth, and C. W. Carlson, Interaction between electrostatic whistlers and electron holes in the auroral region, *J. Geophys. Res.*, 107(A12), 1463, doi:10.1029/2002JA009303, 2002.

### 1. Introduction

[2] Observations by the Fast Auroral Snapshot (FAST) spacecraft [Carlson *et al.*, 1998a] have shown that quasi-static parallel electric fields were responsible for the generation of magnetic field-aligned accelerated electrons in the auroral region of the magnetosphere [Carlson *et al.*, 1998b]. From a theoretical viewpoint the existence of such parallel electric fields in the collisionless auroral plasma can be understood as a macroscopic consequence of the wave-particle interactions which allow space charge separation to take place microscopically. Therefore the study of these complex, small-scale, and often nonlinear interactions is of major importance for our understanding of auroral physics.

[3] The distinction between the upward current region, which is located above the aurora, and the downward, or return current region is fundamental to classifying these various wave-particle interactions. In the return current region the response of the ionosphere to magnetospheric perturbations generates parallel electric fields which accelerate electrons of ionospheric origin upwards. FAST obser-

vations have shown that these field-aligned electron beams have little thermal spread across the magnetic field and that they form a plateaued distribution along the magnetic field [Carlson *et al.*, 1998b].

[4] The low-altitude orbit of the FAST spacecraft (below 4200 km) and the high-time resolution of its plasma and field instruments led to the discovery of positive solitary potential structures (also called electron holes) [Ergun *et al.*, 1998] associated with the upgoing electron beams. They are similar to the electric potential spikes observed by the GEOTAIL and POLAR spacecraft at higher altitude in the polar cap and in the plasma sheet boundary layer [Matsumoto *et al.*, 1994; Mozer *et al.*, 1997; Franz *et al.*, 1998; Cattell *et al.*, 1999]. The amplitude of the spikes observed at low altitude by FAST (up to 1 V/m in extreme cases) is, however, much larger than the one observed at higher altitude by the other satellites. The parallel and perpendicular electric fields take the form of bipolar and monopolar spikes, respectively. These waveforms are obtained by a set of two double probe antennas which are sounding a spheroidal potential structure moving upwards along the magnetic field **B**. The speed of the solitary potential structures inferred from the time delay of the signal measured by the two antennas is of the order of a few thousand kilometers

per second. The width of these structures is several Debye lengths, or equivalently several hundred meters [Ergun *et al.*, 1998].

[5] These structures have been modeled as one-dimensional (1-D) electron phase-space holes along magnetic field lines [Muschiatti *et al.*, 1999a], which are stationary solutions of the Vlasov-Poisson equations in a fast-moving reference frame. They are a specific form of Bernstein-Green-Kruskal equilibrium [Bernstein *et al.*, 1957] maintained by the electron dynamics while the ions form a homogeneous neutralizing background due to the high speed of the hole compared with the ion-thermal and ion-acoustic velocities. Electrons of negative energy are trapped inside the positive potential structure while electrons with positive energy are just passing through the structure. Prescribing the shape of the electric potential and the distribution function of passing electrons, one constructs the trapped electron distribution function which satisfies Vlasov-Poisson equations [Muschiatti *et al.*, 1999a].

[6] The generation mechanism of these structures is not yet clear even if several 2-D and 3-D simulations suggest that they emerge from the strongly nonlinear interaction between bidirectional electron beams [see e.g., Goldman *et al.*, 1999]. 2-D simulations have shown that electron holes are grossly unstable for conditions where the bounce frequency of the trapped electrons along the magnetic field line  $\omega_b$  is larger than their gyrofrequency  $\Omega_e$  [Muschiatti *et al.*, 2000]. However, in the highly magnetized auroral plasma where  $\Omega_e \gg \omega_b$ , one can expect the electron holes to live for at least several bounce periods. Still, as demonstrated by 2-D particle-in-cell (PIC) simulations [Oppenheim *et al.*, 1999] and Vlasov simulations [Newman *et al.*, 2001] with periodic boundary conditions, we cannot preclude a weak instability of the electron holes relative to specific types of perturbations. Furthermore, 3-D PIC simulations have shown that the eventual decay of electron holes was accompanied by the emission of lower-hybrid waves [Singh *et al.*, 2000; Oppenheim *et al.*, 2001].

[7] A potential candidate for the destabilization of electron holes are the electrostatic whistler wave (EWW) emissions which are a common feature of the auroral zone [André, 1997]. Their frequency range extends from the lower-hybrid frequency up to the electron plasma frequency, the lower-hybrid wave being the low frequency and high perpendicular wave number limit of this mode. As long as the frequency of EWW is large compared with the lower-hybrid frequency, their dispersion relation reduces to  $\omega = \omega_{pe} \cos \theta$ , where  $\omega_{pe}$  is the electron plasma frequency and  $\theta$  is the angle between the wave vector  $\mathbf{k}$  and the magnetic field  $\mathbf{B}$ . Among these emissions is the well-known auroral hiss which has both electrostatic and electromagnetic components. However, auroral hiss is believed to be generated by incoherent Cerenkov emission from intense fluxes of precipitating electrons [Beghin *et al.*, 1989] observed in the upward current region. Therefore auroral hiss is a typical feature of these upward current regions. One can also see EWW emitted from downward current regions in the form of VLF saucers or V-shaped VLF hiss emissions seen on frequency-time spectrograms [Gurnett, 1966; Mosier and Gurnett, 1969]. The frequency-time dependence of VLF saucers is due to their dispersion relation and to the localization of their source region [James, 1976].

[8] Observations by the VIKING spacecraft have shown that upgoing electrons were sometimes observed in conjunction with VLF saucers [Lonnqvist *et al.*, 1993]. FAST observations have recently revealed that as much as 85% of VLF saucers were actually associated with upgoing electron fluxes (R. E. Ergun, C. W. Carlson, J. P. McFadden, R. J. Strangeway, M. V. Goldman, and D. L. Newman, FAST observations of VLF saucers, submitted to *Journal of Geophysical Research*, 2001b). However, the suggestion made by James [1976] that cold electron beams might be responsible for the generation of VLF saucers has not been confirmed. Electron distribution functions observed by FAST in the source regions of VLF saucers are indeed plateaued and exhibit a large velocity spread along the magnetic field direction. On the other hand, Ergun *et al.* [2001] found that 79% of the VLF saucer events associated with upgoing electron fluxes had fast solitary waves (electron holes) on their emitting flux tubes. These experimental new results and the fact that simulations often show the presence of EWW in association with electron holes [e.g., Goldman *et al.*, 1999] led us to investigate the interaction of EWW and electron holes in the downward auroral current region. The question whether the EWW, which might be generated through this interaction, do or do not take the form of VLF saucers is left for future work.

[9] In this paper we try to answer the question of whether electron holes may or may not excite EWW. While Singh *et al.* [2001] considered the Cerenkov emission of EWW by the moving charge distribution of an electron hole, we study the resonant amplification of an EWW through its interaction with the particles which are supporting the electron hole structure. We first describe the physics of the well-known Landau resonance between passing (nontrapped) electrons and the EWW using Newtonian mechanics. By close analogy this mechanical method is adapted for trapped particles whose undisturbed motion is periodic along the magnetic field line. The Hamiltonian formalism of action-angle variables is used and canonical perturbation theory allows us to identify the bounce resonance of trapped particles with the wave. We calculate the growth rate of EWW, compare our result with the one recently obtained by Vetoulis and Oppenheim [2001], and apply it to typical FAST observations. Finally, we summarize our results and underline some of the questions which are still open to future work.

## 2. Landau Resonance of Passing Particles

[10] The electron hole is a stationary solution of the 1-D Vlasov-Poisson equations. It is defined by  $F_0(x, v) = F_p(x, v) + F_h(x, v)$ , the distribution function of passing and trapped electrons taken in the direction parallel to the magnetic field, which self-consistently sustains the positive localized potential structure defined by  $\Phi_0(x)$ . This BGK equilibrium moves along the magnetic field at a constant velocity of the order of the electron thermal velocity.

[11] Let us perturb this equilibrium with a monochromatic electrostatic whistler wave (with frequency  $\omega$  and parallel wave number  $k_{\parallel}$ ) defined by

$$\delta\Phi(x, t) = (\delta\Phi_0/2) \exp[i(k_{\parallel}x - \omega t)] + C.C. \quad (1)$$

where *C.C.* stands for complex conjugate hereafter. In the highly magnetized auroral plasma, electrons are tied tightly to their magnetic field line such that the perpendicular component of the whistler wave vector only introduces a constant phase shift in equation (1) which has been included in the complex wave amplitude  $\delta\Phi_0$ . It is well known that the wave undergoes strong linear Landau damping if its parallel phase velocity  $\omega/k_{\parallel}$  is close to the electron thermal speed of the distribution. Only a small number of particles, whose velocity is of the order of the wave phase velocity, take part in this resonant process. This is why the physics of linear Landau damping can be described by first looking at the energy exchange between one electron and the wave and then by averaging this effect over the small class of particles which efficiently interact with the wave. In this approach, particles are uncorrelated and a purely mechanical treatment of Landau damping can be carried out [c.f. *Baumjohann and Treumann*, 1996, p. 256]. We now describe this method in some detail because of its close similarity to the method we will develop in the next section for the interaction between trapped particles and EWW.

[12] Passing particles with positive energy have free orbits in phase space ( $x, v$ ). Their undisturbed motion is, to be sure, modified by the potential structure associated with the electron hole, but as long as the time they spend crossing one hole is much smaller than the average transit time spent between two consecutive structures along a magnetic field line, they should mainly interact with the wave via Landau resonance. The energy change of one passing electron with initial velocity  $v$  after interaction with the wave over a time  $t$  can be written as

$$\Delta E(t) = \frac{1}{2}m(v + \Delta v)^2 - \frac{1}{2}mv^2 \sim mv\Delta v. \quad (2)$$

Integrating the equation of motion, one has to evaluate the variation of the electron momentum

$$m\Delta v = - \int_0^t e\delta E \sin[k_{\parallel}X(t')] dt', \quad (3)$$

where  $X(t') = x(t') - \omega t'/k_{\parallel}$  is the position of the electron in the wave reference frame,  $m$  and  $-e$  are the mass and charge of the electron, and  $\delta E \sin[k_{\parallel}X(t')] = -\partial(\delta\Phi)/\partial x$  is the wave electric field along the magnetic field. This can be easily achieved by iterating the integration of equation (3) in order to approximate the perturbed electron trajectory  $X(t')$  at lowest order in  $\delta E$ . The next step is to average  $\Delta E(t)$  over all initial phases of the electron relative to the wave phase. It can be shown that

$$\langle \Delta v(t) \rangle = \left( \frac{e\delta E}{m} \right)^2 \frac{1}{k_{\parallel}^2 V^3} \left[ \cos(k_{\parallel} Vt) - 1 + \frac{1}{2}(k_{\parallel} Vt) \sin(k_{\parallel} Vt) \right], \quad (4)$$

where  $V \equiv dX/dt$  is the electron velocity in the wave reference frame. This implies that the interaction is resonant for particles with a velocity  $V \sim 0$ , i.e.  $v \sim \omega/k_{\parallel}$ . Under the linearity assumption, the distribution function remains

unchanged over time  $t$  and the global energy density loss or gain for the passing electrons is given by

$$\delta W_p(t) = \int_{-\infty}^{+\infty} m(V + \omega/k_{\parallel}) \langle \Delta v(t) \rangle F_p(V + \omega/k_{\parallel}) dV. \quad (5)$$

Since only resonant particles play a significant role in this integral,  $F_p$  can be approximated by using a Taylor expansion around  $\omega/k_{\parallel}$ :

$$F_p(V + \omega/k_{\parallel}) = F_p(\omega/k_{\parallel}) + V(\partial F_p/\partial V)_{V=0} + \dots \quad (6)$$

Because of the parity of  $\langle \Delta v(t) \rangle$ , the term proportional to  $\int \omega/k_{\parallel} \langle \Delta v(t) \rangle F_p(\omega/k_{\parallel}) dV$  vanishes. Provided that the distribution function is not too flat around  $\omega/k_{\parallel}$ ,  $\delta W_p(t)$  is approximated by

$$\delta W_p(t) \sim m(\omega/k_{\parallel}) (\partial F_p/\partial V)_{V=0} \int V \langle \Delta v(t) \rangle dV \quad (7)$$

which, after integration with equation (14), becomes

$$\delta W_p(t) \sim -\frac{\pi}{2} \left( \frac{e\delta E}{m} \right)^2 \frac{m\omega}{k_{\parallel}^2} (\partial F_p/\partial V)_{V=0} t. \quad (8)$$

The secular variation of  $\delta W_p(t)$  implies an exponential damping or growth of the wave amplitude. The dependence of equation (8) on the slope of the distribution function  $(\partial F_p/\partial V)_{V=0}$  shows that the damping or growth of the wave depends on how many particles have a velocity which is smaller or larger than the wave phase velocity. In that sense, a wave-plasma system at Landau resonance behaves like a mechanical system where slow particles get accelerated by the wave while fast particles are decelerated by it as one would expect in an elastic collision.

### 3. Hamiltonian Approach for Trapped Particles

[13] The other particles which contribute to the energy exchange with the wave are trapped in the potential structure  $\Phi_0(x)$ . They have closed orbits in phase-space and their unperturbed motion is periodic with a bounce frequency  $\omega_b(E)$ : they oscillate between two turning points  $x_{\pm}$  for which  $E = -e\Phi_0(x_{\pm})$ . We will now proceed by close analogy with the procedure we described in some detail for Landau resonance. We first have to calculate the energy  $\Delta E(t) = \Delta[\frac{1}{2}mv^2 - e\Phi_0(x)]$  given to one trapped particle by the wave after a time  $t$ , assuming we switch on the wave at time  $t = 0$ . Newton's equation of motion cannot be solved iteratively as in section 2, where the effect of the potential structure has been neglected. We have to adopt a new set of variables in which the complex but periodic motion of trapped electrons will be more naturally described.

[14] For this purpose, we introduce the Hamiltonian formalism of action-angle variables. Hamilton equations can be first written for canonical variables  $(x, p)$  with  $p$  as the momentum. The Hamilton function reads

$$H(p, x, t) = \frac{p^2}{2m} - e\Phi_0(x) - e\delta\Phi(x, t) \equiv H_0(x, p) - e\delta\Phi(x, t). \quad (9)$$

## Electron hole / VLF wave Interaction

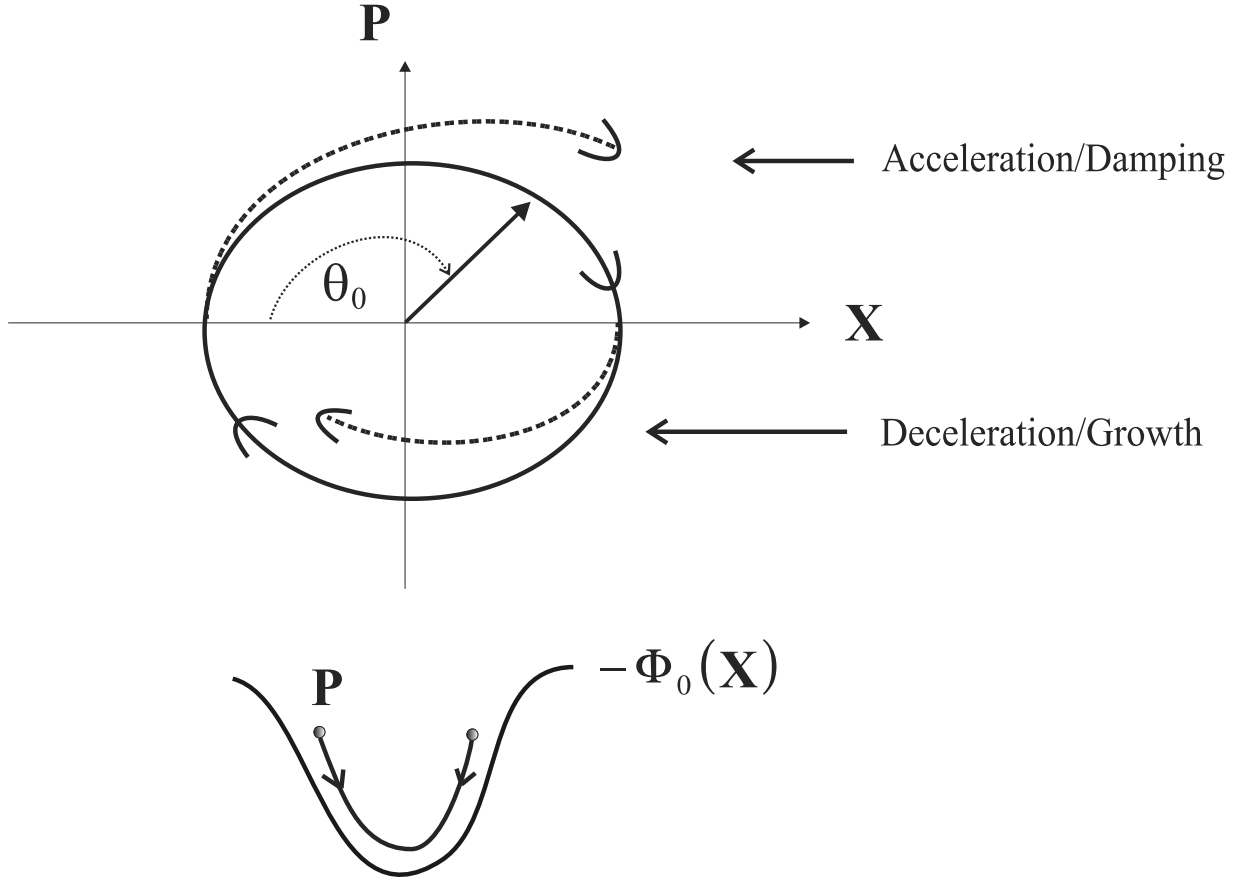


**Figure 1.** Sketch of the interaction between particles trapped in the electrostatic potential of the electron hole,  $\Psi_0(x)$ , and the whistler wave. The electron trajectory takes the form of a closed orbit in phase space  $(x, p)$ . Action-angle variables  $(I_0, \theta_0)$  are an equivalent set of canonically conjugate variables with the angle  $\theta_0$  defined from an arbitrarily chosen origin:  $\theta_0(t = 0) = \phi$ . The wave perturbs the electron orbits. The initial electron phase  $\phi$  determines if the particle is accelerated or decelerated, which contributes to either damping or growth of the initial perturbation.

Following page 129 of *Landau and Lifchitz* [1964], new canonical variables for the unperturbed electron trajectory are defined by introducing the generating function

$$S_0(x, I_0) = \int p(x, I_0) dx, \quad (10)$$

where the adiabatic invariant  $I_0$  is the action variable given by

$$I_0 = \frac{1}{2\pi} \oint p dx. \quad (11)$$

This constant of motion corresponds to the area delimited by closed orbits of trapped electrons in phase space  $(x, p)$ . A sketch of such orbit is given in Figure 1, where the electron position is defined by an angle variable  $\theta_0$ . Action is a

function of energy  $E$  only and one easily shows from Hamilton equations that  $dI_0/dE = 1/\omega_b(E)$ . Considering  $(\theta_0, I_0)$  as new canonical variables, the transformation equations relating new to old variables are defined by

$$\begin{aligned} p &= \partial S_0(x, I_0) / \partial x \\ \theta_0 &= \partial S_0(x, I_0) / \partial I_0. \end{aligned} \quad (12)$$

[15] The generating function  $S_0$  does not explicitly depend on time, which implies that the new Hamilton function reduces to the old one in terms of the new variables, namely to  $E = H_0(I_0)$ . Hamilton equations state that

$$\begin{aligned} dI_0/dt &= -\partial H_0 / \partial \theta_0 = 0 \\ d\theta_0/dt &= \partial H_0 / \partial I_0 = \omega_b(E), \end{aligned} \quad (13)$$



from which we conclude that  $\theta_0 = \omega_b(E)t + \phi$  behaves as an angle variable with initial value  $\phi$ . Indeed, after one bounce period,  $\theta_0$  increased by  $2\pi$  and any function of  $I_0$  and  $\theta_0$  (or equivalently of  $x$  and  $p$ ) is therefore periodic in  $\theta_0$  with a period  $2\pi$ .

[16] When the perturbation is switched on, we can define a new set of action-angle variables  $(\theta, I)$ . The generating function  $S(x, I, t) = \int p(x, I, t)dx$  does depend on time and the new Hamilton function  $H$  is an explicit function of  $I, \theta$ , and  $t$ . The time dependency of  $H$  implies that the electron orbit in phase space is no longer closed, or equivalently that both the electron energy and the action variable  $I$  vary along the electron trajectory. The expression for the new Hamilton function is  $H(I, \theta, t) = H_0(I) - e\delta\Phi(I, \theta, t) + \partial S/\partial t$ . Owing to the smallness of the perturbation  $\delta\Phi$ , we know, however, that the trajectory of most trapped electrons will be only slightly distorted by the wave. If we define a small amplitude parameter  $\varepsilon \propto \delta\Phi/\Phi_0 \ll 1$ , the variation of the generating function  $\partial S/\partial t$  will be of first order in  $\varepsilon$ . We can neglect this term in the Hamilton function  $H$  because it will not bring any resonant contribution to the energy exchange between particles and waves. Within this perturbative context, the new Hamilton function can be cast into the form

$$H(I, \theta, t) = H_0(I) + \varepsilon\Psi(I, \theta, t). \quad (14)$$

Action-angle variables for trapped electrons can be expanded in a power series in  $\varepsilon$  around their undisturbed value  $(\theta_0, I_0)$  according to

$$\begin{aligned} I &= I_0 + \varepsilon I_1 + \varepsilon^2 I_2 + \dots \\ \theta &= \theta_0 + \varepsilon \theta_1 + \varepsilon^2 \theta_2 + \dots \end{aligned} \quad (15)$$

The consistency of this expansion is guaranteed by imposing Hamilton equations

$$\begin{aligned} dI/dt &= -\partial H/\partial \theta \\ d\theta/dt &= +\partial H/\partial I, \end{aligned} \quad (16)$$

which we solve for  $(I, \theta)$  order-by-order in  $\varepsilon$  [see e.g., *Sagdeev et al.*, 1988, p. 56].

[17] This perturbation procedure allows us to evaluate the energy gained or lost by an electron,  $\Delta E(\phi, I_0, t)$ , whose initial position in phase-space is defined by  $\phi$  and  $I_0$ . Under the linearity condition, we assume that over the time  $t$  of interest the amplitude of the electrostatic potential  $\Phi_0(x)$  does not vary. Taylor expanding  $H_0$  around  $I_0$  to second order in  $\varepsilon$  leads to

$$\Delta E(\phi, I_0, t) \equiv \Delta[H_0(I)] \sim \varepsilon\omega_b I_1 + \varepsilon^2\omega_b \left( I_2 + \frac{1d\omega_b}{2dE} I_1^2 \right). \quad (17)$$

In order to solve Hamilton equations, we need to express the perturbation  $\delta\Phi(x, t)$  as a function of  $I, \theta$ , and  $t$ . We approximate the electron motion as an harmonic oscillator in the potential well  $-\Phi_0(x) \sim -\Phi_0(1 - x^2/2\alpha^2)$  where  $\Phi_0$  is the potential amplitude and  $\alpha$  its characteristic width. Note that this approximation is best for deeply trapped electrons. It implies that  $x(\theta) \sim \Lambda_E \sin \theta$  where  $\Lambda_E = x_+ - x_-$

is the distance between turning points at energy  $E$ . Introducing Bessel functions  $J_n$ , for which  $J_{-n} = (-1)^n J_n$ , we can write the perturbation as

$$\begin{aligned} \Psi(I, \theta, t) &= \frac{B}{2} \left( \sum_{n=1}^{\infty} J_n(k_{\parallel}\Lambda_E) \{ \delta\Phi_0 \exp[i(n\theta - \omega t)] \right. \\ &\quad \left. + (-1)^n \delta\Phi_0^* \exp[i(n\theta + \omega t)] \} \right. \\ &\quad \left. + \delta\Phi_0 \exp(-i\omega t) \right) + C.C., \end{aligned} \quad (18)$$

with  $B = -e/\varepsilon$  and  $\delta\Phi_0^* \equiv C.C.(\delta\Phi_0)$ . By using this approximation we do not have to know the exact form of the BGK equilibrium. The function  $\Psi(I, \theta, t)$  takes the form of a Fourier series in  $\theta$ , which correctly describes the fact that the undisturbed motion of electrons is periodic in  $\theta$ . We shall see in the following section that this periodicity is the key element of the physics we have to describe in our model. This is why the use of the Hamiltonian formalism of action-angle variables is fully justified in this study.

## 4. Growth Rate of Electrostatic Whistlers

### 4.1. Integration of Hamilton Equations

[18] At first order in  $\varepsilon$  equation (16) yields

$$\begin{aligned} \frac{dI_1}{dt} &= -i \frac{B}{2} \sum_{n=1}^{\infty} n J_n(k_{\parallel}\Lambda_E) A_n(\theta_0, t) + C.C. \\ \frac{d\theta_1}{dt} &= I_1 \left( \frac{d^2 H_0}{dI^2} \right)_{I_0} + \frac{B}{2} \left[ \sum_{n=1}^{\infty} \frac{dJ_n(k_{\parallel}\Lambda_E)}{dI_0} A_n(\theta_0, t) \right. \\ &\quad \left. + \frac{dJ_0(k_{\parallel}\Lambda_E)}{dI_0} \delta\Phi_0 \exp(-i\omega t) \right] + C.C., \end{aligned} \quad (19)$$

where

$$A_n(\theta_0, t) = \delta\Phi_0 \exp[i(n\theta_0 - \omega)t] + (-1)^n \delta\Phi_0^* \exp[i(n\theta_0 + \omega)t]. \quad (20)$$

Note that the undisturbed motion of electrons is present in these equations through the angle variable  $\theta_0 = \omega_b t + \phi$ . After time integration and with  $\delta\Phi_0 \equiv |\delta\Phi_0| \exp(i\psi)$ , we obtain

$$\begin{aligned} I_1 &= -B|\delta\Phi_0| \sum_{n=1}^{\infty} n J_n(k_{\parallel}\Lambda_E) \\ &\quad \cdot \left( \frac{\{ \cos[(n\omega_b - \omega)t + n\phi + \psi] - \cos(n\phi + \psi) \}}{(n\omega_b - \omega)} + (-1)^n P_n \right), \end{aligned} \quad (21)$$

where  $P_n$  is equal to the first term in the parentheses with the substitution  $(\omega, \phi) \rightarrow (-\omega, -\phi)$ . The first term of  $I_1$  is resonant when  $n\omega_b(E_R) - \omega = 0$  whereby the energy gain or loss, given by equation (17), will be important at a given frequency  $\omega$  for those electrons whose energy  $E_R$  satisfies

this relation. Keeping only resonant terms in equation (19) after time integration, we also have

$$\begin{aligned} \theta_1 = & -B|\delta\Phi_0|\omega_b \frac{d\omega_b}{dE} \sum_{n=1}^{\infty} n J_n(k_{\parallel}\Lambda_E) \\ & \cdot \left( \frac{\{\sin[(n\omega_b - \omega)t + n\phi + \psi] - \sin(n\phi + \psi)\}}{(n\omega_b - \omega)^2} \right. \\ & - \frac{\cos(n\phi + \psi)}{(n\omega_b - \omega)} t + B|\delta\Phi_0| \sum_{n=1}^{\infty} \frac{dJ_n(k_{\parallel}\Lambda_E)}{dI_0} \\ & \cdot \left. \left( \frac{\{\sin[(n\omega_b - \omega)t + n\phi + \psi] - \sin(n\phi + \psi)\}}{(n\omega_b - \omega)} \right) \right). \end{aligned} \quad (22)$$

Some of the nonresonant terms of  $\theta_1$  do give resonant contributions to  $I_2$ , but we have checked that these terms do not survive the next step of the calculation (i.e., the average over phase space).

[19] At second order in  $\varepsilon$  we only need  $I_2$ , which is obtained from the time integration of

$$\begin{aligned} \frac{dI_2}{dt} = & B|\delta\Phi_0| \sum_{n=1}^{\infty} n^2 J_n(k_{\parallel}\Lambda_E) \theta_1 \{\cos[(n\omega_b - \omega)t + n\phi + \psi] \\ & + (-1)^n \cos[(n\omega_b + \omega)t + n\phi - \psi]\} \\ & + B|\delta\Phi_0| \sum_{n=1}^{\infty} n \frac{dJ_n(k_{\parallel}\Lambda_E)}{dI_0} I_1 \\ & \times \{\sin[(n\omega_b - \omega)t + n\phi + \psi] \\ & + (-1)^n \sin[(n\omega_b + \omega)t + n\phi - \psi]\} \end{aligned} \quad (23)$$

and which includes several other resonant contributions to  $\Delta E(\phi, I_0, t)$  in equation (17).

#### 4.2. Average Over Phase-Space

[20] We can consider, as in section 2 for Landau resonance, that the distribution function of trapped particles  $F_t(x, v)$  is not affected by the bounce resonance over the timescale of the linear instability. Therefore we can average  $\Delta E(x, v, t) \equiv \Delta E(x, E, t) = \Delta E(\phi, I_0, t)$  over all initial positions and energies of trapped electrons such that the global energy given to the particles by the wave reads

$$\delta W_t(t) = \oint dx \int_{-e\Phi_0}^0 \frac{dE}{mv} F_t(E) \Delta E(x, E, t). \quad (24)$$

The domain of integration covers the whole spectrum of energy for trapped electrons. Note that by construction of the BGK equilibrium,  $F(x, v)$  is a function of the energy only,  $F_t(E)$ . We can permute the integrals and, with the substitution  $dx/v = dt'$ , see that the integration over all initial positions is equivalent to an integration over all initial phases  $\phi$ , such that

$$\delta W_t(t) = \frac{1}{m} \int_{-e\Phi_0}^0 \frac{dE}{\omega_b(E)} F_t(E) \int_0^{2\pi} \Delta E[\phi, I_0(E), t] d\phi. \quad (25)$$

Performing the integration over  $\phi$ , we see that  $\langle \varepsilon \omega_b I_1 \rangle_{\phi} = 0$  because  $\int_0^{2\pi} \cos(n\phi) d\phi = 0$  for any  $n \neq 0$ . This means that

at first order, while some electrons gain energy from the wave, others loose energy in the same amount depending on their initial phase, as can be seen in Figure 1. This result is also similar to the one obtained for Landau damping, where the energy exchange between particles and waves only exists at second order in the wave perturbation. Lengthy calculations (not reproduced here) show that the only resonant terms of equation (17) which survive the integration over  $\phi$  give

$$\langle \Delta E \rangle_{\phi} = e^2 |\delta\Phi_0|^2 \pi \omega_b^2(E) \frac{d\omega_b}{dE} \sum_{n=1}^{\infty} C_n(E), \quad (26)$$

where

$$C_n(E) = n^3 J_n^2(k_{\parallel}\Lambda_E) \left\{ \frac{2[\cos(\delta\omega_n t) - 1]}{\delta\omega_n^3} + \frac{t \sin(\delta\omega_n t)}{\delta\omega_n^2} \right\}, \quad (27)$$

with  $\delta\omega_n = n\omega_b(E) - \omega$ . The terms proportional to  $dJ_n(k_{\parallel}\Lambda_E)/dE$  all vanish in the integration process. Note the similarity between equation (4) and equations (26) and (27).

[21] As in section 2 for Landau resonance, we expand  $F_t(E)$  around the resonant energy  $E_R$

$$F_t(E) \sim F_t(E_R) + (E - E_R)(dF_t/dE)_{E_R} + \dots \quad (28)$$

Provided that there is no resonance overlap in the energy or frequency domain, we transform the energy integral of  $\delta W(t)$  into a sum of resonant integrals of the form

$$\begin{aligned} \delta W_t(t) \sim & \frac{e^2 |\delta\Phi_0|^2 \pi}{m} \sum_{n=1}^{\infty} \int_{E_R - \beta_R}^{E_R + \beta_R} \left[ F_t(E_R) + (E - E_R)(dF_t/dE)_{E_R} \right] \\ & \cdot \omega_b(E) \frac{d\omega_b}{dE} C_n(E) dE. \end{aligned} \quad (29)$$

Introducing the new variable  $E^* = E - E_R$ , we can extend the integration domain from  $[E_R - \beta_R, E_R + \beta_R]$  to  $[-\infty, +\infty]$  without affecting the result owing to the rapid decrease of the integrand far from the resonance. With the relation  $\delta\omega_n = nE^*(d\omega_b/dE)_{E_R}$ , we have

$$\begin{aligned} \delta W_t(t) \sim & \frac{e^2 |\delta\Phi_0|^2 \pi}{m} \sum_{n=1}^{\infty} n^3 \int_{-\infty}^{+\infty} \left[ F_t(E_R) + E^* (dF_t/dE)_{E_R} \right] \\ & \cdot J_n^2(k_{\parallel}\Lambda_E) \omega_b \frac{d\omega_b}{dE} \left\{ \frac{2}{n^3 E^{*3}} (d\omega_b/dE)_{E_R}^{-3} \right. \\ & \cdot \left[ \cos(nE^*(d\omega_b/dE)_{E_R} t) - 1 \right] \\ & \left. + \frac{t \sin(nE^*(d\omega_b/dE)_{E_R} t)}{n^2 E^{*2}} (d\omega_b/dE)_{E_R}^{-2} \right\} dE^*. \end{aligned} \quad (30)$$

Similarly to the Landau case, the parity of the term in brackets  $\{\cdot\}$  shows that only the derivative of  $F_t(E)$  is important because the other term vanishes. Approximating the factor  $J_n^2(k_{\parallel}\Lambda_E) \omega_b d\omega_b/dE$  by its value at resonant energy

and using  $\chi = |n(d\omega_b/dE)_{E_R}|E^*$  as integration variable, we can explicitly calculate the integral

$$\delta W_t(t) \sim -t \frac{e^2 |\delta \Phi_0|^2 \pi \omega}{m} \sum_{n=1}^{\infty} J_n^2(k_{\parallel} \Lambda_{E_R}) \frac{(dF_t/dE)_{E_R}}{|(d\omega_b/dE)_{E_R}|}. \quad (31)$$

Note the secular variation of this quantity resulting from the bounce resonance of electrons with the wave. In addition, we point out that it has the physical dimensions of an energy density integrated over a column of length unity along the magnetic field.

### 4.3. Conservation of Energy

[22] Electron holes appear in trains distributed along the magnetic field lines. Let  $L$  be the average length between two consecutive electron holes. Then  $\delta W_t L^{-1}$  represents the energy density exchanged between electrons trapped in the holes and the wave. Thus by energy conservation the total wave energy density  $W_W$  satisfies the relation

$$\frac{\delta W_p(t) + \delta W_t(t)/L}{t} = - \frac{dW_W}{dt}. \quad (32)$$

Note that electron holes do not need to be periodically spaced along the magnetic field lines. The total wave energy density along the magnetic field is  $2W_W = \epsilon_0 k^2 |\delta \Phi_0|^2 S_{yz}$  for electrostatic whistler waves, where  $S_{yz}$  is the elementary surface in the plane perpendicular to the magnetic field. Defining the complex frequency of the perturbation as  $\omega + i\gamma$ , we have  $[\delta W_p(t) + \delta W_t(t)/L]/t = -2\gamma W_W$ . The normalized growth or damping rate of the wave is given by

$$\gamma/\omega = \frac{\pi \omega_{pe}^2}{k^2 L} \sum_{n=1}^{\infty} J_n^2(k_{\parallel} \Lambda_{E_R}) \frac{(df_t/dE)_{E_R}}{|(d\omega_b/dE)_{E_R}|} + \frac{\pi \omega_{pe}^2}{2k^2} (df_p/dv)_{\omega/k_{\parallel}}, \quad (33)$$

where  $f_{p,t} = F_{p,t}/(n_0 S_{yz})$  is the electron distribution function normalized to unity when  $x \rightarrow \infty$  and  $n_0$  is the density. We point out that equation (32) implies that trapped and passing electrons form two distinct classes of particles, an assumption which means that we do not consider the time evolution of the BGK equilibrium. Such a nonlinear evolution of the electron hole might in fact result from this resonant instability on a timescale longer than the instability timescale  $\gamma^{-1}$ .

## 5. Application to Fast Observations

### 5.1. Electron Hole Model

[23] In order to apply our theoretical results to FAST observations, we first need to consider a specific model of the undisturbed electron hole. Hereafter, we use standard dimensionless units where length is normalized to the electron Debye length  $\lambda_{De}$ , velocity to the electron thermal velocity  $v_e \equiv \sqrt{T_e/m}$ , potential to  $T_e/e$ , and energy to the electron thermal energy  $mv_e^2/2$ . In these units, we have  $E = v^2 - 2\Phi_0$ . We use the following Gaussian profile  $\Phi_0(x)$  as a reasonably good fit to the spatial variation of the electrostatic potential in the direction parallel to the magnetic field:

$$\Phi_0(x) = \Psi \exp(-x^2/2\Delta^2). \quad (34)$$

Following *Muschiatti et al.* [1999b], as a first step we assume the drift of the passing electrons to be zero in the frame of the fast-moving electron hole. In this frame, the distribution function of passing particles with energy  $E > 0$  can be qualitatively approximated by

$$f_p(E) = \frac{6\sqrt{2}}{\pi(8 + E^3)}. \quad (35)$$

After integration of Vlasov-Poisson equations, the distribution function of trapped electrons with energy  $-2\Psi < E < 0$  reads

$$f_t(E) = \frac{\sqrt{-E}}{\pi \Delta^2} \left[ 1 + 2 \ln \left( \frac{\Psi}{-2E} \right) \right] + \frac{6 + (\sqrt{2} + \sqrt{-E})(1 - E)\sqrt{-E}}{\pi(\sqrt{2} + \sqrt{-E})(4 - 2E + E^2)}. \quad (36)$$

For the total distribution function not to be negative at its minimum where  $E = -2\Psi$ , the half-width  $\Delta$  of the potential defined by equation (34) must exceed a minimum value  $\Delta_m$  defined by

$$\Delta_m^2 = 4(4 \ln 2 - 1) \sqrt{\Psi} (1 + \sqrt{\Psi}) \frac{1 + \sqrt{\Psi} + \Psi}{3 + 4\sqrt{\Psi} + 2\Psi}. \quad (37)$$

### 5.2. Numerical Results

[24] Figure 2a displays the contour plot of the growth rate of EWW from their interaction with the particles trapped in an electron hole defined by  $\Psi = 0.4$  and  $\Delta = \Delta_m$ . The growth rate, which is given in percents of the wave frequency  $\omega$ , is a function of frequency and wave number normalized to  $\omega_{pe}$  and  $\lambda_{De}^{-1}$ , respectively. Landau damping has not been included here and the electron hole drift relative to the electron distribution function,  $\delta v$ , is zero. The contribution from the first harmonic of the bounce frequency, the  $n = 1$  term in equation (33), is given by solid contour lines. The dashed contour lines correspond to  $n = 2$ . Contributions from higher-order harmonics are negligible in this case. In Figure 2b, Landau damping from passing electrons is included according to equation (33) and, as expected, large wave number waves are heavily damped. Waves emitted at  $n = 2$ , which are associated with larger wave numbers owing to the Bessel factor  $J_2^2(k_{\parallel} \Lambda_{E_R})$  in (33), are therefore only marginally amplified by the resonance. The emission process turns out to be efficient in the 0.15–0.4  $\omega_{pe}$  frequency range. Normalized growth rates, up to 9% here, are typical of an efficient linear instability.

[25] As suggested by FAST observations, however, electron holes drift upwards faster than does the plateaued electron distribution function. It implies that the emission at the harmonics of the bounce frequency is Doppler shifted in the reference frame of the electron distribution such that

$$\omega = n\omega_{b0} + k_{\parallel} \delta v. \quad (38)$$

Typical electron hole drifts are of the order of the electron thermal velocity. Figures 2c and 2d include this Doppler

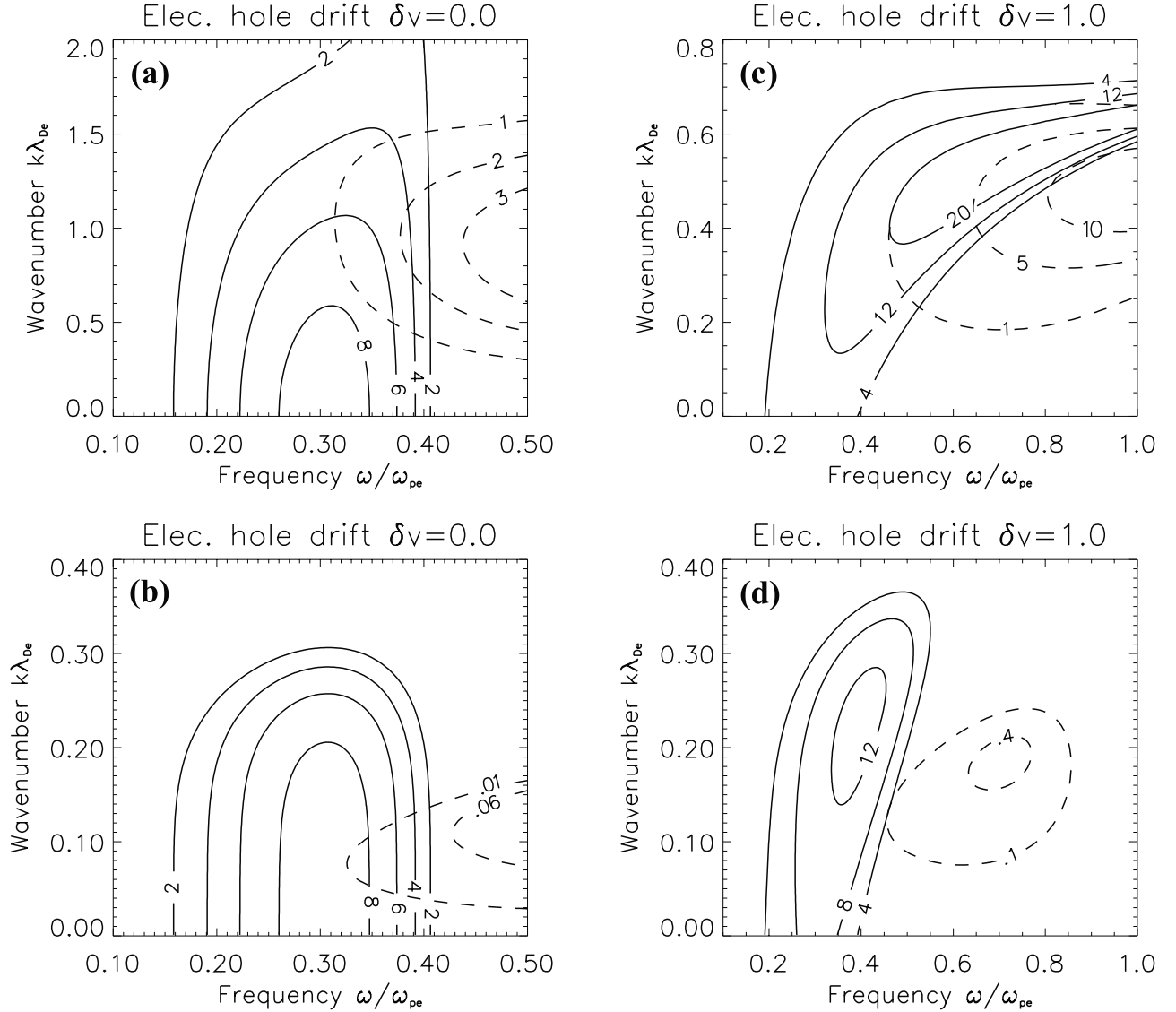


**Figure 2.** Growth rate in percent of the wave frequency versus normalized wave number and frequency for electron hole drift  $\delta v = 0$  and  $\delta v = 1$ . The solid (dashed) contours give the  $n = 1$  ( $n = 2$ ) term of equation (43).  $\Psi = 0.4$  and  $\Delta = \Delta_m$ . Figures 2a and 2c do not include Landau damping while lower ones Figures 2b and 2d do.

effect (here  $\delta v = 1$ ) in the growth rate of EWW with and without the Landau damping term, respectively. Higher-frequency waves than before can be excited, up to  $\sim 0.7\omega_{pe}$ , and the maximum growth rate increases. Second harmonic generated waves are more easily excited as well. This is partly due to the attenuation of the Landau damping at higher parallel phase velocity. In addition the Bessel factor in equation (33) combines with the Doppler frequency shift in such a way that the growth rate does not monotonically decrease with wave number. Instead, there is a nonzero wave number which maximizes the growth rate and this wave number increases with frequency.

[26] Figure 3 shows how the growth rate varies with the electron hole amplitude  $\Psi$ . Here we have fixed  $\delta v = 1$  and  $\Delta = \Delta_m$ . As before, the upper panels do not include the Landau damping term while the lower ones do. Some of the contours are interrupted because we set a maximum value,

$E_M = -e\Psi/20$ , for the energy of trapped electrons: we do not consider infinite parallel excursions of trapped electrons in the electrostatic potential, which provides a lower limit  $\omega_{b0}(E_M)$  for the bounce frequency. The maximum energy  $E_M$  is also used to set the value of the repetition parameter of electron holes,  $L$  in equation (33), to  $3\Lambda_{E_M}$ . In agreement with the hypothesis of no resonance overlap that we used to obtain equation (29), the motion of particles near the separatrix of the electron hole is therefore not considered in this model. It can be seen that the instability strengthens when  $\Psi$  increases and that it spreads in frequency-wave number space as well. In Figure 3d, emissions at the second harmonic of the bounce frequency exist up to the electron plasma frequency. Landau damping is however an important stabilizing factor for the electron hole, particularly at small wavelength and high frequency. In the same format as before, Figure 4 displays, for  $\delta v = 1$  and  $\Psi = 0.4$ , the growth



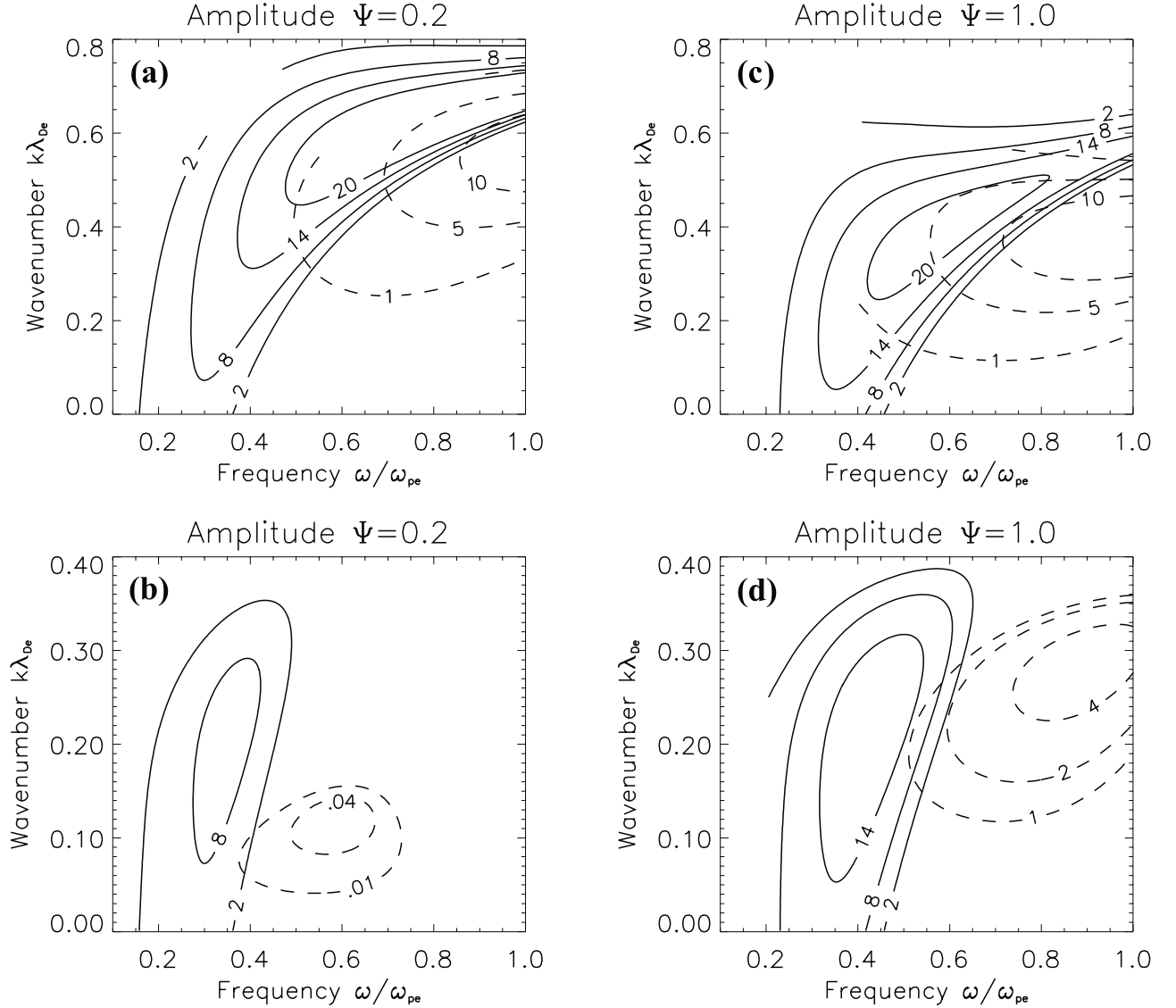


**Figure 3.** Same format as Figure 2 for  $\delta v = 1$ ,  $\Delta = \Delta_m$ , and two values of the electron hole amplitude  $\Psi$ . Contours are interrupted for bounce frequencies of particles near the separatrix of the electron hole.

rate as a function of the electron hole half-width  $\Delta$ . Wider structures, which have smaller bounce frequencies, excite lower frequency EWW. The growth rate, however, weakens in this case, from  $\sim 12\%$  when  $\Delta = \Delta_m$ , down to  $\sim 3\%$  when  $\Delta = 3\Delta_m$ .

[27] In conclusion, Figures 2 through 4 show that the bounce resonance instability is efficient in a large frequency range, from the lowest frequencies, possibly from the lower-hybrid frequency, up to the electron plasma frequency, depending on the properties of the electron holes. Note that EWW observed by FAST in the auroral region covers this whole frequency range [Ergun *et al.*, 2001]. Typical parameters for the electron holes observed by FAST [Ergun *et al.*, 1998] are  $\Psi \sim 0.2\text{--}0.6$ ,  $\Delta \sim 1.5\text{--}3\Delta_m$ , and  $\delta v \sim 0.6\text{--}1$ . Growth rates up to  $\sim 2\text{--}3\%$  can be obtained at low frequency  $\omega/\omega_{pe} \sim 0.1$  and small wave numbers  $k\lambda_{De} \sim 0.25$  with these parameters. The parallel wave phase velocity is  $(k\lambda_{De})^{-1}$  times  $v_e$ . Therefore we expect the existence of low-frequency EWW with large parallel phase velocity in

the region where such electron holes are observed. Note that such high parallel wave phase velocities would not be expected from a classical beam-plasma interaction. At higher frequency, the parallel wave phase velocity tends to decrease and the growth rate increases.

## 6. Discussion and Conclusions

[28] The physical mechanism of bounce resonance that we put into evidence here is similar to the one studied in a recent paper by Vetoulis and Oppenheim [2001]. While these authors started from Vlasov-Poisson equations, for which equations (34)–(36) are indeed a stationary solution, we developed an Hamiltonian approach which allowed us to directly follow the energy exchange between particles and waves. The growth rate of EWW, given by equation (33), differs however from equation (14) of Vetoulis and Oppenheim [2001] because we did not use a square box approximation in order to describe the phase space orbit of electrons

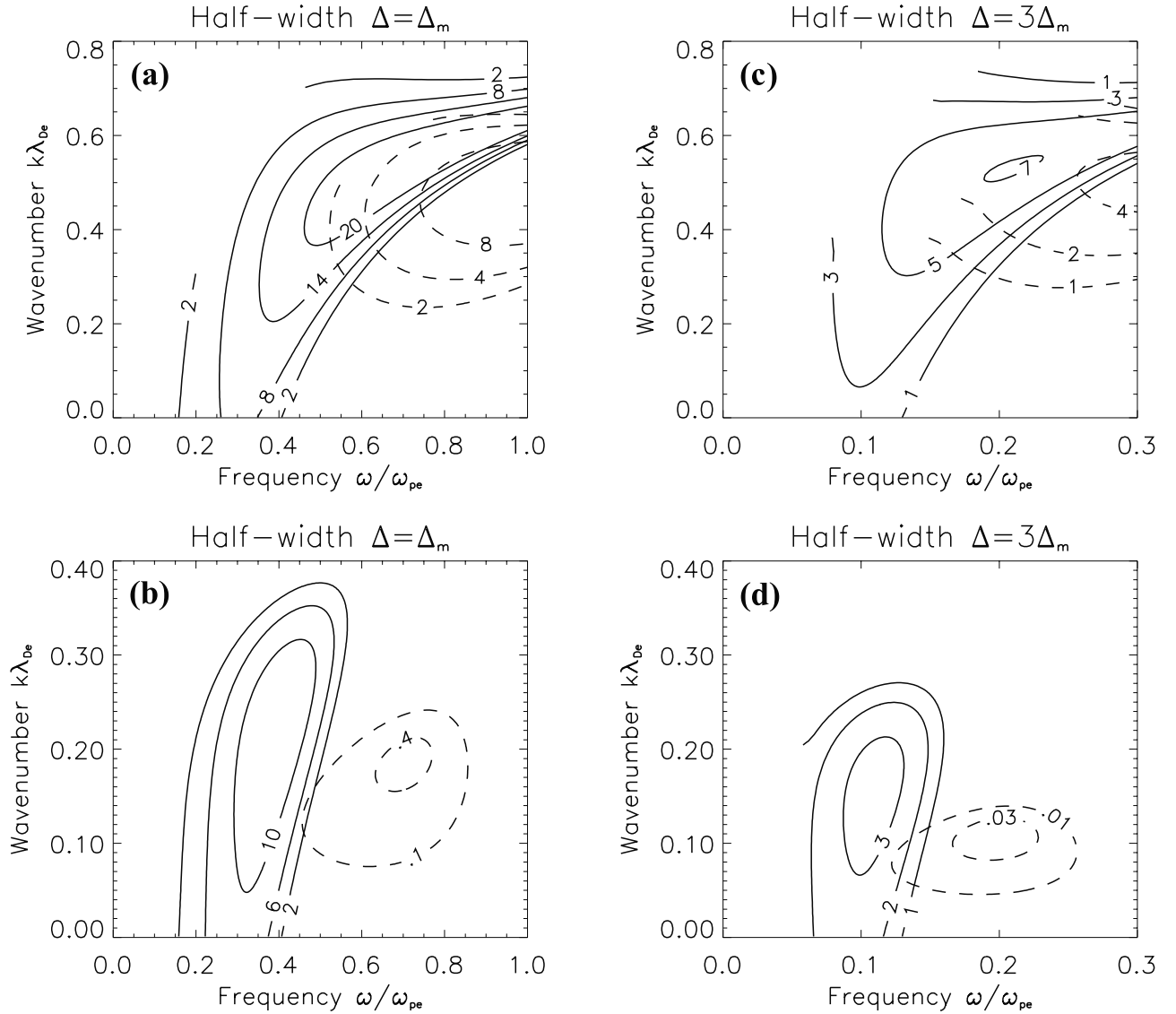


**Figure 4.** Same format as Figures 2 and 3 for  $\delta\nu = 1$ ,  $\Psi = 0.4$ , and two values of the electron hole half-width  $\Delta$ . Note the different frequency range between left and right panels.

at zeroth order in the wave perturbation. Instead, the undisturbed trajectory of trapped electrons is approximated by an harmonic oscillator. As a result we obtained a more accurate description of the growth rate dependence on the wave number. This leads to the Bessel factor  $J_n^2(k_{\parallel}\Lambda_E)$  in equations (18) and (33). Furthermore, we have introduced the effect on the growth rate of the Doppler frequency shift related to electron hole motion. We have shown that this effect was very important and partly controlled by the Bessel factor.

[29] The parametric study and comparison to FAST data also allowed us to understand how the bounce resonance could excite EWW over their whole frequency spectrum. By contrast, an alternate mechanism to generate EWW, proposed by Newman *et al.* [2001], is only efficient in the lower part of the frequency spectrum. In this other mechanism, electron holes are unstable to oblique EWW whose frequency is an order of magnitude smaller than the bounce frequency. This time scale ordering is necessary in order to perform time averaging of relevant equations over the

bounce period. These two mechanisms might be however complementary because typical growth rates obtained from the bounce resonance tend to weaken at low frequency. As suggested by Singh *et al.* [2001], the 3-D structure of electron holes might also play an important role in the emission process; these authors have shown that the spontaneous emission of EWW is controlled by the parallel and perpendicular scaling of electron holes and by plasma magnetization. The 3-D nature of electron holes might be important for the emission of EWW by bounce resonance as well, and we plan to use our Hamiltonian approach in order to study these effects.

[30] In conclusion, we have performed a theoretical analysis of the interaction between EWW and electron holes. We have developed a Hamiltonian approach which allowed us to consider a relevant set of action-angle variables to study the energy exchange between EWW and electrons trapped in the electrostatic potential associated with the electron hole. Using canonical perturbation theory,

we found that this energy exchange was resonant when the harmonics of the bounce frequency of trapped electrons match the frequency of the perturbation. Then, by averaging this effect over all initial phases and energies of the electrons trapped in an electron hole and by considering a train of electron holes propagating up the magnetic field line, we estimated the growth rate of EWW. Application to FAST observations showed that this linear instability is able to generate EWW over the whole frequency spectrum of these waves, from the lower-hybrid frequency up to the electron plasma frequency with a growth rate varying from a few percents at low frequency up to  $\sim 10\%$  at higher frequency. In addition, predictions have been made that the parallel phase velocity of EWW emitted by this process can be large compared to the electron thermal velocity.

[31] **Acknowledgments.** M.B. thanks R. Pottelette (Centre d'étude des Environnements Terrestre et Planétaires) and R. A. Treumann (Max-Planck Institut für Extraterrestrische Physik) for their encouragement. This research is part of the France-Berkeley program. This work was supported by NASA grant NAG5-3596.

[32] Shadia Rifai Habbal thanks Jolene S. Pickett and Nagendra Singh for their assistance in evaluating this paper.

## References

- André, M., Waves and wave-particle interactions in the auroral region, *J. Atmos. Terr. Phys.*, **59**, 1687–1712, 1997.
- Baumjohann, W., and R. A. Treumann, *Basic Space Plasma Physics*, Imperial Coll. Press, London, 1996.
- Beghin, C., J. L. Rauch, and J. M. Bosqued, Electrostatic plasma waves and HF auroral hiss generated at low altitude, *J. Geophys. Res.*, **94**, 1359–1378, 1989.
- Bernstein, I. B., J. M. Greene, and M. D. Kruskal, Exact nonlinear plasma oscillations, *Phys. Rev.*, **108**, 546–550, 1957.
- Carlson, C. W., R. F. Pfaff, and J. G. Watzin, The Fast Auroral Snapshot (FAST) mission, *Geophys. Res. Lett.*, **25**, 2013–2016, 1998a.
- Carlson, C. W., et al., FAST observations in the downward auroral current region: Energetic upgoing electron beams, parallel potential drops, and ion heating, *Geophys. Res. Lett.*, **25**, 2017–2020, 1998b.
- Cattell, C. A., et al., Comparisons of Polar satellite observations of solitary wave velocities in the plasma sheet boundary and the high-altitude cusp to those in the auroral zone, *Geophys. Res. Lett.*, **26**, 425–428, 1999.
- Egun, R. E., et al., Fast satellite observations of large-amplitude solitary structures, *Geophys. Res. Lett.*, **25**, 2041–2044, 1998.
- Egun, R. E., M. V. Goldman, D. L. Newmann, C. W. Carlson, J. P. McFadden, and R. J. Strangeway, Electron phase-space holes and the VLF saucer source region, *Geophys. Res. Lett.*, **28**, 3805–3808, 2001.
- Franz, J. R., P. M. Kintner, and J. S. Pickett, Polar observations of coherent electric field structures, *Geophys. Res. Lett.*, **25**, 1277–1280, 1998.
- Goldman, M. V., M. M. Oppenheim, and D. L. Newman, Nonlinear two-stream instabilities as an explanation for auroral bipolar wave structures, *Geophys. Res. Lett.*, **26**, 1821–1824, 1999.
- Gurnett, D. A., A satellite study of VLF hiss, *J. Geophys. Res.*, **71**, 5599–5615, 1966.
- James, H. G., VLF saucers, *J. Geophys. Res.*, **81**, 501–514, 1976.
- Landau, L. D., and E. M. Lifchitz, *Mechanics*, p. 129, MIR, Moscow, 1964.
- Lonnqvist, H., M. Andre, L. Matson, A. Bahnsen, L. G. Blomberg, and R. E. Erlandson, Generation of VLF saucer emissions observed by the Viking satellite, *J. Geophys. Res.*, **98**, 13,565–13,574, 1993.
- Matsumoto, H., H. Kojima, T. Miyatake, Y. Omura, M. Okada, I. Nagano, and M. Tsutsui, Electrotastic solitary waves (ESW) in the magnetotail: BEN wave forms observed by GEOTAIL, *Geophys. Res. Lett.*, **21**, 2915–2918, 1994.
- Mosier, S. R., and D. A. Gurnett, VLF measurements of the poynting flux along the geomagnetic field with the Injun 5 satellite, *J. Geophys. Res.*, **74**, 5675–5687, 1969.
- Mozer, F. S., R. Ergun, M. Temerin, C. Cattell, J. Dombeck, and J. Wygant, New features of time domain electric-field structures in the auroral acceleration region, *Phys. Rev. Lett.*, **79**, 1281–1284, 1997.
- Muschietti, L., R. E. Ergun, I. Roth, and C. W. Carlson, Phase-space electron holes along magnetic field lines, *Geophys. Res. Lett.*, **26**, 1093–1096, 1999a.
- Muschietti, L., I. Roth, R. E. Ergun, and C. W. Carlson, Analysis and simulation of BGK electron holes, *Nonlinear Proc. Geophys.*, **6**, 211–219, 1999b.
- Muschietti, L., I. Roth, C. W. Carlson, and R. E. Ergun, Transverse instability of magnetized electron holes, *Phys. Rev. Lett.*, **85**, 94–97, 2000.
- Newman, D. L., M. V. Goldman, M. Spector, and F. Perez, Dynamics and instability of electron phase-space tubes, *Phys. Rev. Lett.*, **86**, 1239–1242, 2001.
- Oppenheim, M., D. L. Newman, and M. V. Goldman, Evolution of electron phase-space holes in a 2D magnetized plasma, *Phys. Rev. Lett.*, **83**, 2344–2347, 1999.
- Oppenheim, M., G. Vetoulis, D. L. Newman, and M. V. Goldman, Evolution of electron phase-space holes in 3d, *Geophys. Res. Lett.*, **28**, 1891–1894, 2001.
- Sagdeev, R. Z., D. A. Usikov, and G. M. Zaslavsky, *Nonlinear Physics: From the Pendulum to Turbulence and Chaos*, Hardwood Acad., New York, 1988.
- Singh, N., S. M. Loo, B. E. Wells, and C. Deverapalli, Three-dimensional structure of electron holes driven by an electron beam, *Geophys. Res. Lett.*, **27**, 2469–2472, 2000.
- Singh, N., S. M. Loo, and B. E. Wells, Electron hole as an antenna radiating plasma waves, *Geophys. Res. Lett.*, **28**, 1371–1374, 2001.
- Vetoulis, G., and M. Oppenheim, Electrostatic mode excitation in electron holes due to wave bounce resonances, *Phys. Rev. Lett.*, **86**, 1235–1238, 2001.

M. Berthomier, J. W. Bonnell, C. W. Carlson, L. Muschietti, and I. Roth, Space Sciences Laboratory, University of California, Berkeley, CA 94720-7450, USA. (matthieu@ssl.berkeley.edu; jbonnell@ssl.berkeley.edu; cwc@ssl.berkeley.edu; laurent@ssl.berkeley.edu; ilan@ssl.berkeley.edu)